

Response and Uncertainty of the Parabolic Variance PVAR to Noninteger Exponents of Power Law

François Vernotte¹, Siyuan Chen², and Enrico Rubiola³

Abstract—The oscillator fluctuations are described as the phase or frequency-noise spectrum or in terms of a wavelet variance as a function of the measurement time. The spectrum is generally approximated with the “power law,” i.e., a Laurent polynomial with integer exponents of the frequency. This article provides: 1) the analytical expression of the response of the wavelet variance parabolic variance (PVAR) to the frequency-noise spectrum in the general case of noninteger exponents of the frequency and 2) a useful approximate expression of the statistical uncertainty. In turn, PVAR is relevant in that it replaces the widely used modified Allan variance (MVAR), featuring the identification of noise processes with fewer data.

Index Terms—Degrees of freedom (dof), fractional noise, frequency stability, uncertainty assessment.

I. INTRODUCTION

THE fluctuations of an oscillator are generally described as the phase noise $\mathcal{L}(f)$, where f is the Fourier frequency, or as the two-sample variance $\sigma_y^2(\tau)$, where τ is the integration time. The latter takes different flavors, the most known of which are the Allan variance (AVAR) and the modified Allan variance (MVAR). The concepts related to $\mathcal{L}(f)$ were introduced in the 1960s to describe the fast fluctuations of oscillators for radars and frequency synthesis [1]. By contrast, $\sigma_y^2(\tau)$ was introduced to describe the fluctuations of Cs-beam clocks for timekeeping, with obvious focus on slow fluctuations [2], [3]. Traditionally, the boundary between these two choices

was $\tau \approx 0.1, \dots, 1$ or $f \approx 1, \dots, 10$ Hz, with small overlap, of the order of one decade. In fact, time counters could not be easily used at a sampling interval τ_0 smaller than ≈ 100 ms, limited by the slowness of the IEEE 488 BUS transferring American Standard Code for Information Interchange (ASCII) data. By contrast, the measurement of $\mathcal{L}(f)$ at low Fourier frequencies was limited by the narrow dynamic range of the double balanced mixer used as the phase-to-voltage converter (no more than $\pm 20^\circ$) and of the analog-to-digital converters. The Fast Fourier Transform analyzers were so complex and expensive that they were avoided when possible. Interestingly, the two-sample variance is broadly equivalent to a one-octave filter centered at $f \approx 0.45/\tau$.

Nowadays, these limitations are gone, and the overlap in the domain of application of $\mathcal{L}(f)$ and $\sigma_y^2(\tau)$ is of 6–8 decades. Digital instruments can measure $\mathcal{L}(f)$ from 0.1 to 1 mHz [4]–[7]. This is made possible by software-defined radio techniques (see [8], [9] for a general overview), which enables phase measurements not bounded to $\pm\pi$. The CORDIC algorithm [10], [11] is the preferred choice to calculate $\varphi(t)$ from the digitized I/Q stream. Counters with picosecond resolution were available since the 1970s with the Nutt interpolator [12], but continuous time stamps at a sampling interval $\tau_0 \approx 100$ ns [13], [14] could be possible only due to field-programmable gate arrays (FPGAs). The minimum τ is actually greater than τ_0 because trivial limitations intervene, but the practical limit is still of the order of several μ s. The conclusion is that assessing the equivalence between spectra and variances is more important than ever.

It is generally agreed that the phase noise of oscillators is well described by the “power law” or “polynomial law” model, which is the extension of the regular polynomial to negative powers of the variable (Laurent polynomials). While the literature is shy about exceptions, we came across significant practical cases where the phase noise has a noninteger slope over a few decades. In other domains of physics, it is generally agreed that flicker noise has the spectrum of the f^β type, where the exponent β is actually in $[-1.2, -0.8]$ to $[-1.5, -0.5]$, depending on the author [15]–[17]. Accordingly, we may find f^β phase noise or $f^{\beta-2}$ phase noise after the phase-to-frequency conversion known as the Leeson effect [18]. The fractional-order frequency control, nowadays quite popular [19]–[21], is a good reason for noninteger slopes in the spectrum of a locked oscillator or laser. Noninteger slopes also appear in other branches of frequency metrology. For example, theoretical predictions about millisecond pulsars

Manuscript received December 29, 2020; revised March 2, 2021; accepted March 26, 2021. Date of publication April 26, 2021; date of current version April 30, 2021. This work was supported in part by the Agence Nationale de la Recherche (ANR) Program d’Investissement d’Avenir (PIA) through the FIRST-TF Network under Grant ANR-10-LABX-48-01, in part by the Oscillator Instability Measurement Platform (IMP) Project under Grant ANR-11-EQPX-0033-OSC-IMP, in part by the Ecole Universitaire de Recherche (EUR) Engineering and Innovation through Physical Sciences, Hightechnologies, and cross-disciplinary research (EIPHI) Graduate School under Grant ANR-17-EURE-00002, and in part by grants from the Région Bourgogne Franche-Comté intended to support the PIA. The Associate Editor coordinating the review process was Dr. Daniel Belega. (Corresponding author: François Vernotte.)

François Vernotte is with the CNRS (UMR 6174), Time and Frequency Department, FEMTO-ST Institute and the Observatory THETA, University Bourgogne Franche-Comté, 25000 Besançon, France (e-mail: francois.vernotte@femto-st.fr).

Siyuan Chen is with Radioastronomy Station Nançay, PSL, 18330 Nançay, France, also with LPC2E, Université d’Orléans, 45000 Orléans, France, and also with the Time and Frequency Department, FEMTO-ST Institute, University Bourgogne Franche-Comté, 25000 Besançon, France.

Enrico Rubiola is with the CNRS (UMR 6174), Time and Frequency Department, FEMTO-ST Institute and the Observatory THETA, University Bourgogne Franche-Comté, 25000 Besançon, France, and also with the Division of Quantum Metrology and Nanotechnology, Istituto Nazionale di Ricerca Metrologica (INRiM), 10135 Torino, Italy.

Digital Object Identifier 10.1109/TIM.2021.3073721

suggest that the common FM noise could follow the $f^{-7/3}$ law [22], [23]. Finally, a continuous power law is also necessary, especially in Bayesian statistical analysis, if the exponent of this law is a parameter that we are trying to estimate [24].

The response of $\sigma_y^2(\tau)$ to phase noise in the case of noninteger exponents of the power law was already solved [25] for the AVAR and the MVAR, while the parabolic variance (PVAR) was introduced later [26], [27]. MVAR is no longer interesting for us because PVAR is suitable for the same applications, enabling the detection of the same noise phenomena at the same confidence level with a shorter data record [27].

This work stands on [25] and extends the results to PVAR providing conversion formulas, degrees of freedom (dofs), and statistical uncertainty (Type A uncertainty, according to the definitions given by the International Vocabulary of Metrology [28]).

II. RESPONSE TO POLYNOMIAL SPECTRA

A. Basic Definitions and Tools

We consider a clock signal $V_0 \cos[\omega_0 t + \varphi(t)]$ of nominal frequency $\omega_0/2\pi$ and random phase $\varphi(t)$. It is understood that $\varphi(t)$ is not bounded to $\pm\pi$ and that $|\dot{\varphi}(t)| \ll \omega_0$. The associated time fluctuation is $\mathbf{x}(t) = \varphi(t)/\omega_0$, usually referred to as phase time. The quantity $\mathbf{y}(t) = \dot{\mathbf{x}}(t)$ is the fractional frequency fluctuation.

According to the IEEE Standard 1139 [29], the phase noise is defined as $\mathcal{L}(f) = (1/2)S_\varphi(f)$, that is, half the single-sided power spectral density (PSD) of $\varphi(t)$. For our purposes, it is convenient to let $S_\varphi(f)$ aside and to use the quantity

$$S_y(f) = \frac{f^2}{(\omega_0/2\pi)^2} S_\varphi(f) \quad (1)$$

which provides fully equivalent information. The associated polynomial law is usually written as

$$S_y(f) = \sum_{\alpha=-2}^2 h_\alpha f^\alpha \quad (2)$$

where the exponent α equals -2 for random walk FM noise, -1 for flicker FM noise, 0 for white FM noise, 1 for flicker PM noise, and 2 for white PM noise.

From a general perspective, the two-sample variance can be written as

$$\sigma_y^2(\tau) = \frac{1}{2} \mathbb{E} \left\{ [\bar{y}_2 - \bar{y}_1]^2 \right\} \quad (3)$$

where $\mathbb{E}\{\}$ is the mathematical expectation and \bar{y}_1 and \bar{y}_2 stand for $\mathbf{y}(t)$ averaged over contiguous time intervals of duration τ (hereafter the integration time). Our use of (3) differs from the general literature in that \bar{y}_2 and \bar{y}_1 are weighted averages. The uniform average gives AVAR, the triangular average gives MVAR, and the parabolic average gives PVAR. Other options are possible, for example, the Hadamard and the Picimbono variances. Accordingly, (3) is rewritten as

$$\sigma_y^2(\tau) = \mathbb{E} \left\{ \left[\int_{-\infty}^{\infty} \mathbf{y}(t) w(t) dt \right]^2 \right\} \quad (4)$$

where $w(t)$ is a wavelet-like function that describes $\bar{y}_2 - \bar{y}_1$, including the weight functions. The specific $w(t)$, named

$w_A(t)$ for AVAR, $w_M(t)$ for MVAR, and $w_P(t)$ for PVAR, is defined in [27, Fig. 3 and related text]. For example, the PVAR weighting function is

$$w_P(t) = \frac{3\sqrt{2}t}{\tau^3} (|t| - \tau) \quad (5)$$

with $t \in [-\tau, \tau]$ which is the quadratic form which gives the parabolic shape of this weighting function. Since $\mathbf{y}(t)$ is the derivative of $\mathbf{x}(t)$, (4) may be rewritten as

$$\sigma_y^2(\tau) = \mathbb{E} \left\{ \left[\int_{-\infty}^{\infty} \mathbf{x}(t) \dot{w}(t) dt \right]^2 \right\} \quad (6)$$

where $\dot{w}(t)$ is the time derivative of $w(t)$. Thus, for PVAR

$$\dot{w}_P(t) = \frac{6\sqrt{2}}{\tau^3} \left(|t| - \frac{\tau}{2} \right) \quad (7)$$

with $t \in [-\tau, \tau]$.

In measurements, the variance is calculated from a stream of N samples \mathbf{x}_j taken at the interval τ_0 , and the measurement time is $\tau = m\tau_0$, where m (hereafter the normalized integration time) is an integer. The expectation is replaced with the average $\langle \rangle_M$ on M realizations of $\bar{y}_2 - \bar{y}_1$, and $\sigma_y^2(\tau)$ is replaced with AVAR(τ) or PVAR(τ)

$$\text{AVAR}(\tau) = \frac{1}{2M} \sum_{i=0}^{M-1} [\bar{y}_{i+1} - \bar{y}_i]^2 \quad (8)$$

$$\text{PVAR}(\tau) = \frac{72}{Mm^2\tau^2} \times \sum_{i=0}^{M-1} \left[\sum_{k=0}^{m-1} \left(\frac{m-1}{2} - k \right) (\mathbf{x}_{i+k} - \mathbf{x}_{i+m+k}) \right]^2 \quad (9)$$

and $M = N - 2m$ because $w(t)$ spans over $2m$ samples. The main advantage of PVAR lies in the fact that this linear weighting of the \mathbf{x}_j samples is equivalent to a linear regression and thus provides the best determination of its slope in the sense of least squares. PVAR(τ) is therefore an estimator of the variance of the slope of the \mathbf{x}_j samples over the duration τ . For a more detailed description of PVAR and its properties, see [27] (particularly Fig. 1 and the related text for the linear regression equivalence).

B. Response of AVAR and PVAR to f^α

The response of a generic $\sigma_y^2(\tau)$ to $S_y(f)$ is

$$\sigma_y^2(\tau) = \int_0^\infty |H(f)|^2 S_y(f) df \quad (10)$$

where $H(f)$ is the transfer function or

$$\sigma_y^2(\tau, \alpha) = \int_0^\infty |H(f)|^2 h_\alpha f^\alpha df \quad (11)$$

for the α th term of the polynomial law (2). Using the subscript A for AVAR, $|H(f)|^2$ becomes

$$|H_A(f)|^2 = \frac{2 \sin^2(2\pi f \tau)}{(\pi f \tau)^2} \quad (12)$$

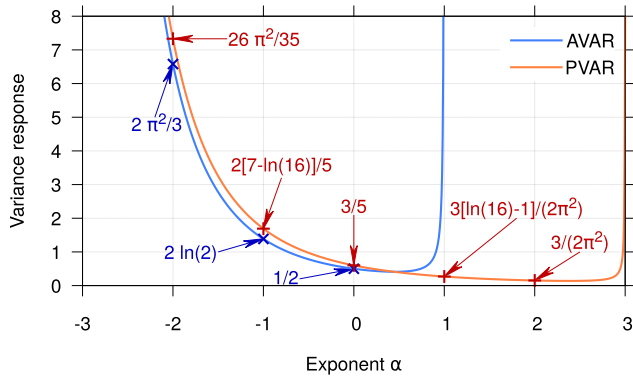


Fig. 1. Continuous response of AVAR and PVAR compared to the known responses for $\alpha \in [-3, +3]$. The responses of AVAR are not plotted for $\alpha \geq 1$ because this estimator diverges without the introduction of a high cutoff frequency.

therefore

$$\text{AVAR}(\tau, \alpha) = \frac{(2^{-\alpha+1} - 4)\Gamma(\alpha - 1) \sin(\pi\alpha/2)}{(2\pi\tau)^{\alpha+1}} h_\alpha. \quad (13)$$

This is equivalent to [25, eq. (14)] because we have not introduced in (10) the usual cutoff frequency f_H .

Similarly, the transfer function associated with PVAR is

$$|H_P(f)|^2 = \frac{9[2 \sin^2(\pi f \tau) - \pi \tau f \sin(2\pi f \tau)]}{2(\pi f \tau)^6} \quad (14)$$

which is (17) of [27], repeated here. Combining (11) and (14), we derive the response of PVAR

$$\text{PVAR}(\tau, \alpha) = 9 \times 2^{5-\alpha} \left[\alpha^2 - \alpha - 4 - 2^\alpha(\alpha - 3) \right] \times \frac{\Gamma(\alpha - 5) \sin(\pi\alpha/2)}{(2\pi\tau)^{\alpha+1}} h_\alpha. \quad (15)$$

Because PVAR converges for f^α from f^{-2} to f^{+2} FM noise, we can assume that (15) is valid for $\alpha \in [-3, +3]$.

Fig. 1 shows the AVAR and PVAR calculated as above, as a function of α . For integer α , the results are the same as in [27, Table I].

III. DEGREES OF FREEDOM OF PVAR ESTIMATES

First, we have to find a simplified expression of the number of dof of PVAR estimates for integer power-law noises. Since this equation was solved for a white PM noise (see (24) in [27]), we assume that the following expression should have the same form:

$$\nu \approx \frac{35}{A(\alpha)m/M - B(\alpha)(m/M)^2} \quad (16)$$

where $A(\alpha)$ and $B(\alpha)$ are coefficients to be determined. After [27, eq. (24)], we already know that $A(+2) = 23$ and $B(+2) = -12$. We determined $A(\alpha)$ and $B(\alpha)$ after massive Monte Carlo simulations and verified the results by comparing them to the dof computed for continuous power law.

A. Determination of the Coefficients From Monte Carlo Simulations

The Monte Carlo simulation was performed by computing 10000 sequences of frequency deviations for each $\alpha \in \{-2, -1, 0, +1, +2\}$ and for each data-run length $N \in \{128, 2048, 32768\}$, i.e., 150000 simulated sequences. For given α , N , and τ , we derived the dof from the averages and the variances of the PVAR for the corresponding set of sequences by using the following well-known property of χ_v^2 distributions [27]:

$$\nu = 2 \frac{\mathbb{E}^2[\text{PVAR}(\tau)]}{\mathbb{V}[\text{PVAR}(\tau)]} \quad (17)$$

where $\mathbb{E}[\]$ and $\mathbb{V}[\]$ are the mathematical expectation and the variance of the argument, respectively. The least square fit results in

- 1) $A(-2) \approx 34$, $A(-1) \approx 28$, $A(0) \approx 27$, $A(+1) \approx 27$, and $A(+2) = 23$.
- 2) $B(\alpha) \approx 12$ for all α .

We have then modeled $A(\alpha)$ by the following third-order polynomial and assumed that $B(\alpha) = B$ is constant:

$$A(\alpha) = 27 + \frac{1}{4}\alpha + \frac{5}{14}\alpha^2 - \frac{3}{4}\alpha^3 \\ B = 12. \quad (18)$$

Due to (16) and (18), we are now able to assess the dof of all PVAR estimates whatever the normalized integration time m or the number of samples M .

The top of Fig. 2 compares the dof obtained by the Monte Carlo simulations and by (16) and (18) for all integer types of noise. The agreement is confirmed by the bottom, which shows that the discrepancies are within $\pm 10\%$ except for the very first values of m ($m = 1, 2$).

The model provided by (16) and (18) can be applied to the classical power law, with integer α . Next, we check on its validity as an extension for real $\alpha \in [-3, 3]$ by computing the dof of PVAR.

B. Verification for Continuous Polynomial-Law Noise

The dof can be computed from (17). The mathematical expectation of the response of PVAR is given by (15), and the variance can be computed from (21) and (22) of [27]

$$\mathbb{V}[\text{PVAR}(\tau)] \\ = \frac{2}{M^2} \sum_{i=0}^{M-1} \sum_{j=0}^{M-1} \left[\frac{72}{m^4 \tau^2} \sum_{k=0}^{m-1} \sum_{l=0}^{m-1} \left(\frac{m-1}{2} - k \right) \left(\frac{m-1}{2} - l \right) \right. \\ \left. \left\{ 2R_x[(i+k-j-l)\tau_0] \right. \right. \\ \left. \left. - R_x[(i+k-j-m-l)\tau_0] \right. \right. \\ \left. \left. - R_x[(i+m+k-j-l)\tau_0] \right\} \right]^2 \quad (19)$$

where $R_x(\tau)$ is the autocorrelation function of the phase-time samples $\mathbf{x}(t) = \int_0^t \mathbf{y}(\theta) d\theta$, i.e., $R_x(\tau) = \mathbb{E}\{\mathbf{x}(t)\mathbf{x}(t+\tau)\}$. We used the following continuous expression of $R_x(\tau)$ versus

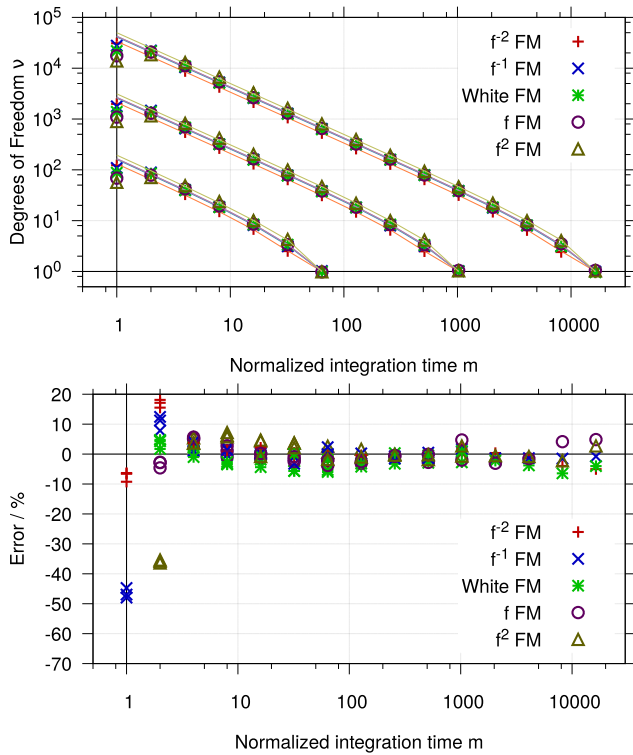


Fig. 2. Top: comparison of the empirical dof (crosses) and the approximations (lines) given by (16) and (18) for all types of noise. The lines are drawn from point to point without interpolation and the last point is set to 1. Bottom: relative difference (in %) between the empirical dof and the approximations.

the power-law exponent α (see [25], [30]):

$$R_x(m\tau_0) = \frac{h_\alpha}{2(2\pi)^\alpha \tau_0^{\alpha-1}} \frac{\Gamma(m - \alpha/2 + 1)\Gamma(\alpha - 1)}{\Gamma(m + \alpha/2)\Gamma(\alpha/2)\Gamma(1 - \alpha/2)}. \quad (20)$$

However, since this expression involves Γ -functions with arguments of the order of m , it limits this computation to $N = 128$ samples ($\Gamma(128) = 3 \cdot 10^{213}$). However, since $\Gamma(z) = (z-1)\Gamma(z-1)$ for $z > 1$, we can rewrite (20) by using the following recurrence formula:

$$\frac{\Gamma(m - \alpha/2 + 1)}{\Gamma(m + \alpha/2)} = \frac{\Gamma(3 - \alpha/2)}{\Gamma(2 + \alpha/2)} \prod_{j=0}^{m-3} \frac{m - j - \alpha/2}{m - 1 - j + \alpha/2}$$

which ensures that the arguments of the Γ functions are greater or equal to 1 for $\alpha \in [-2, +2]$. Therefore, the autocorrelation function may be computed for large N as

$$R_x(m\tau_0) = \frac{h_\alpha}{2(2\pi)^\alpha \tau_0^{\alpha-1}} \frac{\Gamma(3 - \alpha/2 + 1)\Gamma(\alpha - 1)}{\Gamma(2 + \alpha/2)\Gamma(\alpha/2)\Gamma(1 - \alpha/2)} \times \prod_{j=0}^{m-3} \frac{m - j - \alpha/2}{m - 1 - j + \alpha/2}. \quad (21)$$

Due to this equation, we have computed the theoretical variance of PVAR(τ) versus continuous α and deduced the dof from (17).

Let us define $P_\nu(\alpha, m, M) = (35 M/m\nu)$. From (16), we see that $P_\nu(\alpha, m, M) \approx A(\alpha) - Bm/M$. The top of Fig. 3 shows $P_\nu(\alpha, m, M)$ computed from (19) (crosses) and

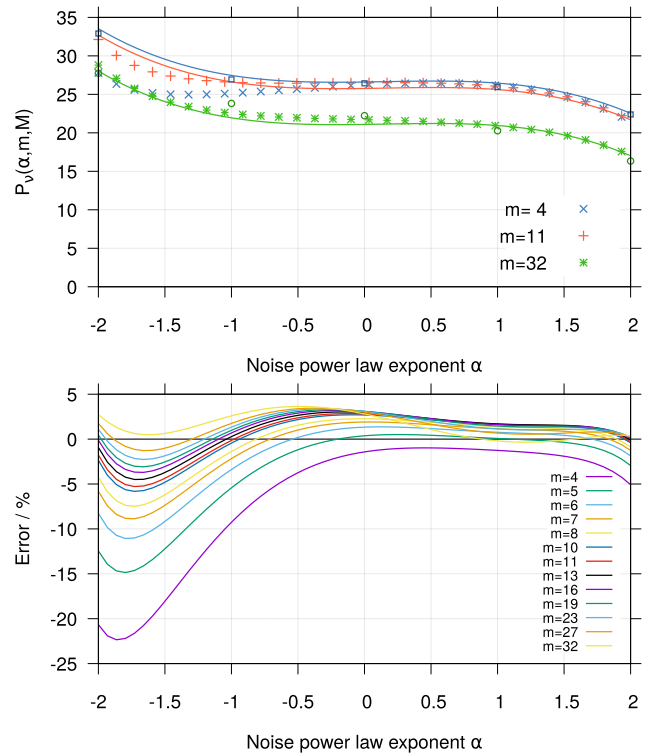


Fig. 3. Top: comparison of $P_\nu(\alpha, m, M)$ computed from (19) (\times , $+$, $*$) and approximated by (16) (solid lines) for $N = 128$ data. The blue squares and the green circles are, respectively, the values obtained for $m = 4$ and $m = 32$ from the Monte Carlo simulations. Bottom: error (in %) between the approximated values of $P_\nu(\alpha, m, M)$ and the computed values.

approximated from (18) (solid lines) versus the noise power law α for $m \in \{4, 11, 32\}$ (we prefer to plot $P_\nu(\alpha, m, M)$ instead of ν because the picture is more readable). The agreement is quite good for $m = 11$ and $m = 16$, but there is a notable difference for $m = 4$ and $\alpha < -1$. The bottom of Fig. 3 shows that this discrepancy is $\approx 20\%$ maximum, but it remains within $\pm 5\%$ in most cases (all α for $m > 8$ and all m for $\alpha > -1$). This agreement is satisfactory to get an acceptable assessment of the PVAR uncertainties since the relative uncertainties are proportional to $1/\sqrt{\nu}$: they are therefore always below 10% and mostly within $\pm 2.5\%$.

C. Case of the Largest Integration Time

The approximation given by (16) and (18) is close enough to the empirical dof ν for $m \leq N/4$. Moreover, we know that $\nu = 1$ for $m = N/2$. This is enough to draw Fig. 2 since no interpolation is performed between the last two points, i.e., $m = N/4$ and $m = N/2$. On the other hand, we note that the approximation diverges beyond $N/4$ (dashed lines in the top of Fig. 4) if intermediate m values are computed. However, it is important to assess the uncertainties within this interval, particularly if N is not a power of 2.

We fill this gap by interpolating the dof within $\text{round}(2^{3/20}N/4) \leq m \leq \text{round}(2^{-3/20}N/2)$ (rounding is necessary to ensure that m is an integer), i.e., between $m_1 \approx \text{round}(1.11 N/4)$ and $m_2 \approx \text{round}(0.901 N/2)$, with the

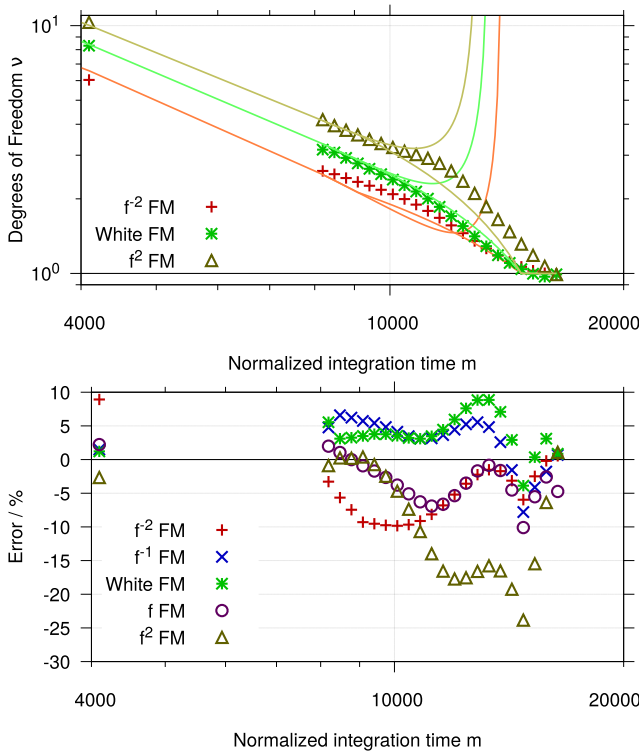


Fig. 4. Top: comparison of the empirical dof (crosses) and the semilogarithmic fits (solid lines) for $N/4 \leq m \leq N/2$ and for random walk FM, white FM, and white PM. The dashed lines represent the approximations given by (16) and (18). In this example, $N = 32\,768$ samples and the logarithmic increment of the m -values is $2^{1/20}$ within $[N/4, N/2]$. Bottom: error (in %) between the empirical dof and the semilogarithmic fits for all types of noise.

following semilogarithmic fit:

$$v(m) = a \ln(m) + b \quad (22)$$

with

$$a = \frac{v(m_1) - 1}{\ln(m_1) - \ln(m_2)} \quad (23)$$

$$b = \frac{\ln(m_1) - v(m_1) \ln(m_2)}{\ln(m_1) - \ln(m_2)}. \quad (24)$$

For $m \geq m_2$, the dofs are set to 1.

Fig. 4 (top) shows an enlargement of the highest two decades of m , i.e., $m \in [4096, 8192]$ for $N = 32\,768$ data, shown to focus on the result of the semilogarithmic fit. The bottom plot shows the error between the fit and the dof computed from the Monte Carlo simulations. Most of these errors are within $\pm 10\%$, except for white FM. In this case of white FM, the error is between $+5\%$ and -20% and up to -24% for $m = 14\,766$. However, this fit is sufficient to ensure an estimation of the PVAR uncertainty for the highest τ within $\sim 10\%$ at worst.

IV. CONCLUSION

From a theoretical calculation, we have determined the response of PVAR for continuous power-law noise spectra. From Monte Carlo simulations, we have obtained a simplified expression providing the dof of the PVAR estimates

within 10% . We have proved that this expression remains valid for noninteger power-law noises. Finally, we have shown that a simple interpolation is efficient to fit the dof for the highest octave of integration times. Due to these results, we will be able to use PVAR to analyze millisecond pulsar timings and to estimate the noninteger exponent of a red noise if it is detected. On the other hand, this article makes it possible to generalize the use of PVAR to process any signal with noninteger power-law noise spectrum.

REFERENCES

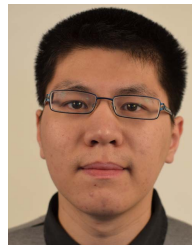
- [1] A. R. Chi, *Short Term Frequency Stability*. Greenbelt, MD, USA: Goddard Space Flight Center, Nov. 1964.
- [2] L. S. Cutler and C. L. Searle, "Some aspects of the theory and measurement of frequency fluctuations in frequency standards," *Proc. IEEE*, vol. 54, no. 2, pp. 136–154, Feb. 1966.
- [3] D. W. Allan, "Statistics of atomic frequency standards," *Proc. IEEE*, vol. 54, no. 2, pp. 221–230, Feb. 1966.
- [4] J. Miles, *TimePod 5330 Programmable Cross Spectrum Analyzer, Operation and Service*. London, U.K.: Miles Design, 2017. [Online]. Available: http://www.miles.io/TimePod_5330A_user_manual.pdf
- [5] Jackson Labs Technologies. *PhaseStation*. Accessed: Nov. 30, 2020. [Online]. Available: <http://www.jackson-labs.com/>
- [6] R. S. GmbH. *FSWP Phase Noise Analyzer and VCO Tester*. Accessed: Nov. 30, 2020. [Online]. Available: <https://www.rohde-schwarz.com>
- [7] G. Feldhaus and A. Roth, "A 1 MHz to 50 GHz direct down-conversion phase noise analyzer with cross-correlation," in *Proc. Europ. Freq. Time Forum*, New York, NY, USA, 2016, pp. 1–5.
- [8] J. Mitola, P. Marshall, K.-C. Chen, M. Mueck, and Z. G. Zvonar, "Software defined radio-20 years later: Part 1," *IEEE Commun. Mag.*, vol. 53, no. 9, pp. 22–23, Sep. 2015.
- [9] J. Mitola, P. Marshall, K.-C. Chen, M. Mueck, and Z. G. Zvonar, "Software defined radio-20 years later: Part 2," *IEEE Commun. Mag.*, vol. 54, no. 1, p. 58, Jan. 2016.
- [10] J. E. Volder, "The CORDIC trigonometric computing technique," *IRE Trans. Electron. Comput.*, vol. 8, no. 3, pp. 330–334, Sep. 1959.
- [11] P. K. Meher, J. Valls, T.-B. Juang, K. Sridharan, and K. Maharatna, "50 years of CORDIC: Algorithms, architectures, and applications," *IEEE Trans. Circuits Syst. I, Reg. Papers*, vol. 56, no. 9, pp. 1893–1907, Sep. 2009.
- [12] R. Nutt, "Digital time intervalometer," *Rev. Sci. Instrum.*, vol. 39, no. 9, pp. 1342–1345, Sep. 1968.
- [13] Carmel Instruments LLC. *Time Interval Analyzers and Frequency counters*. Accessed: Nov. 30, 2020. [Online]. Available: <https://www.carmelinst.com>
- [14] Guidetech. *Continuous Time Interval Analyzers*. Accessed: Nov. 30, 2020. [Online]. Available: <http://www.guidetech.com>
- [15] P. Dutta and P. M. Horn, "Low-frequency fluctuations in solids: $1/f$ noise," *Rev. Mod. Phys.*, vol. 53, no. 3, pp. 497–516, Jul. 1981.
- [16] M. B. Weissman, "1/f noise and other slow, nonexponential kinetics in condensed matter," *Rev. Mod. Phys.*, vol. 60, no. 2, pp. 537–571, Apr. 1988.
- [17] E. Milotti, "Linear processes that produce $1/f$ or flicker noise," *Phys. Rev. E, Stat. Phys. Plasmas Fluids Relat. Interdiscip. Top.*, vol. 51, no. 4, pp. 3087–3103, Apr. 1995.
- [18] E. Rubiola, *Phase Noise and Frequency Stability in Oscillators*. Cambridge, U.K.: Cambridge Univ. Press, 2008.
- [19] Y. Chen, I. Petras, and D. Xue, "Fractional order control—A tutorial," in *Proc. Amer. Control Conf.*, St. Louis, MO, USA, Jun. 2009, pp. 1397–1411.
- [20] I. Petráš, *Fractional-Order Nonlinear System*. Cham, Switzerland: Springer, 2011.
- [21] B. S. Sheard, M. B. Gray, D. E. McClelland, and D. A. Shaddock, "Laser frequency stabilization by locking to a LISA arm," *Phys. Lett. A*, vol. 320, no. 1, pp. 9–21, Dec. 2003.
- [22] E. S. Phinney, "A practical theorem on gravitational wave backgrounds," 2001, *arXiv:astro-ph/0108028*. [Online]. Available: <https://arxiv.org/abs/astro-ph/0108028>
- [23] S. Chen, A. Sesana, and W. Del Pozzo, "Efficient computation of the gravitational wave spectrum emitted by eccentric massive black hole binaries in stellar environments," *Monthly Notices Roy. Astronomical Soc.*, vol. 470, no. 2, pp. 1738–1749, May 2017.

- [24] S. Chen, F. Vernotte, and E. Rubiola, "Applying clock comparison methods to pulsar timing observations," *Monthly Notices Roy. Astronomical Soc.*, vol. 503, no. 3, pp. 4496–4507, May 2021.
- [25] T. Walter, "Characterizing frequency stability: A continuous power-law model with discrete sampling," *IEEE Trans. Instrum. Meas.*, vol. 43, no. 1, pp. 69–79, Feb. 1994.
- [26] E. Benkler, C. Lisdat, and U. Sterr, "On the relation between uncertainties of weighted frequency averages and the various types of Allan deviations," *Metrologia*, vol. 55, no. 4, pp. 565–574, Aug. 2015.
- [27] F. Vernotte, M. Lenczner, P.-Y. Bourgeois, and E. Rubiola, "The parabolic variance (PVAR): A wavelet variance based on the least-square fit," *IEEE Trans. Ultrason., Ferroelectr., Freq. Control*, vol. 63, no. 4, pp. 611–623, Apr. 2016.
- [28] *International Vocabulary of Metrology—Basic and General Concepts and Associated Terms (VIM)*, document JCGM 200:2012, Joint Committee for Guides in Metrology (JCGM), 2012. [Online]. Available: <https://www.bipm.org/en/publications/guides/>
- [29] E. S. Ferre-Pikal, *IEEE Standard Definitions of Physical Quantities for Fundamental Frequency and Time Metrology—Random Instabilities*, Standard 1139-2008, New York, NY, USA, Feb. 2009.
- [30] N. J. Kasdin, "Discrete simulation of colored noise and stochastic processes and $1/f^\alpha$ power law noise generation," *Proc. IEEE*, vol. 83, no. 5, pp. 802–827, May 1995.



François Vernotte received the Ph.D. degree in engineering sciences from the University of Franche-Comté (UFC), Besançon, France, in 1991.

He has been with the Time and Frequency Team, Observatory THETA/UTINAM, UFC, since 1989. His favorite tools are statistical data processing (time series and spectral analysis), parameter estimation (inverse problem and Bayesian statistics), and simulation (Monte Carlo). His current research interest includes long-term stability of oscillators, such as atomic clocks and millisecond pulsars.



Siyuan Chen received the Ph.D. degree from the University of Birmingham, Birmingham, U.K., in 2018.

He has worked on constraining the astrophysics of massive black holes with pulsar timing arrays at the Institute for Gravitational Wave Astronomy, University of Birmingham. He is currently a Post-Doctoral Researcher with the LPC2E, CNRS, Orleans, France, working with the Nancay radio telescope on the precision timing of millisecond pulsars, in particular the data analysis. His research is done with the EPTA and IPTA collaborations. He is also working at the interface between pulsar timing and time-frequency metrology in collaboration with FEMTO-ST, Besançon.



Enrico Rubiola is currently a Professor with the Université de Franche Comté, Besançon, France, a Researcher with the CNRS FEMTO-ST Institute, Besançon, a member of the Observatory of Besançon, and an Associate Researcher with INRiM, Italian Institute of Primary Metrology, Turin, Italy. In 2012, he founded the Oscillator IMP Project, a platform for the measurement of short-term frequency stability and AM/PM noise. In 2013, he founded the European Frequency and Time Seminar, a no-profit crash course in time and frequency,

where he has been chairing and running it since. His primary research interests include high-purity oscillators, AM and PM noise, noise in digital systems, time and frequency metrology, frequency synthesis, Allan variances, microwave photonics, and precision electronics instrumentation. He is known worldwide for his innovative instruments for AM/PM noise measurement with ultimate sensitivity, -210 dBc/Hz and below, for the theory underlying the "Leeson Effect," the theory of modern frequency counters (Π , Λ , and Ω), dedicated signal-processing methods, and hacking oscillators from the phase noise plots.

Prof. Rubiola received the IEEE W. G. Cady Award "for groundbreaking contributions" in the field in 2018.